Allocation of nonbirefringent wear debris: Darkfield illumination associated with PIXE microanalysis reveals cobalt deposition in mineralized bone matrix adjacent to CoCr implants

B. Busse,[1,2] M. Hahn,[1] M. Niecke,[3] B. Jobke,[4] K. Püschel,[5] G. Delling,[6] A. Katzer[7]
[1]*Center for Biomechanics, University Medical Center Hamburg-Eppendorf, Lottestr. 59, D-22529 Hamburg, Germany*
[2]*Center for Musculoskeletal Surgery, Charité-University Medicine Berlin, Free and Humboldt-University of Berlin, Augustenburger Platz 1, D-13353 Berlin, Germany*
[3]*Institute of Experimental Physics, University of Hamburg, Luruper Chaussee 149, D-22761 Hamburg, Germany*
[4]*Musculoskeletal Quantative Imaging Research, Department of Radiology, University of California, San Francisco (UCSF), 505 Parnassus Avenue, San Francisco, California 94143-0628*
[5]*Institute of Legal Medicine, University Medical Center Hamburg-Eppendorf, Martinistr. 52, D-20246 Hamburg, Germany*
[6]*Institute of Bone Pathology, University Medical Center Hamburg-Eppendorf, Lottestr. 59, D-22529 Hamburg, Germany*
[7]*ORTHOCLINIC Hamburg, Oldesloer Straβe 9, D-22457 Hamburg, Germany*

Received 17 March 2007; revised 21 August 2007; accepted 5 October 2007
Published online 9 January 2008 in Wiley InterScience (www.interscience.wiley.com). DOI: 10.1002/jbm.a.31794

Abstract: Abrasive joint replacement material that accumulates in the tissue induces reciprocal effects between prosthesis material and organism. Since the limitations of brightfield and polarized light microscopy for foreign body analysis are well known, a method was applied that ensures the detailed histological assessment of nonbirefringent particles in periprosthetic soft and hard tissue. Cemented and cementless interface regions of five selected autopsy hip implant cases (2 × Endo-Modell Mark III, LINK, 1 × St. Georg Mark II, LINK, Germany; 2 × Spongiosa Metal II, ESKA, Germany) were viewed under darkfield illumination and subsequently analyzed with proton-induced X-ray emission (PIXE). Eight autopsy cases without implants served as controls. Using darkfield illumination technique, metallic particles became visible as luminous points under the microscope. The majority of particles in the samples from the cemented cases were degradation products of radiopaque bone cement. There was minimal evidence of metallic alloy particles in the soft tissues. However, a considerable quantity of heavy metal cobalt (Co) was found in the periprosthetic mineralized bone tissue, which was not observed in the controls. The periprosthetic concentration of cobalt ranged from 38 to 413 ppm. The findings demonstrate a correlation between cobalt concentration, time since implantation, and distance from the implant. Darkfield microscopy associated with PIXE enables a detailed histological assessment of metal particles in the tissue. In an effort to optimize biomechanics, implant design and implantation techniques, the contamination of soft and hard tissue with heavy metal degradation products deserves similar attention in terms of alloy assortment. © 2008 Wiley Periodicals, Inc. J Biomed Mater Res 87A: 536–545, 2008

Key words: bone remodeling; osteoblast; interface; metal ion release; wear debris; cobalt alloy

INTRODUCTION

Formation, transport, and accumulation of degradation products are inevitable phenomena after implantation of prosthetic materials in the human organism. Joint replacements are known to contaminate periarticular tissue and the reticuloendothelial system, with particulate debris and products of ionic corrosion that are not biologically inert. More than two million joint replacements are implanted worldwide every year. Implant loosening and the increasing modularity of many different prosthetic systems result in higher rates of wear debris.[1,2] The enlargement of implant surfaces by means of surface structuring for cementless fixation may be a further factor

Correspondence to: M. Hahn; e-mail: hahn@uke.uni-hamburg.de
Contract grant sponsor: ENDO-Verein – Gemeinnütziger Förderverein ENDO-Stiftung e.V.

leading to increased release and corrosion of metallic elements.[3–5] Joint replacement in a growing number of younger patients means prolonged exposure of the entire organism to these materials and a correspondingly widespread dissemination of wear debris.[6–9]

It is an established fact that wear particles trigger foreign body reactions in the surrounding soft tissue, leading to osteolysis and implant loosening.[10–12] However, already loosened implants show an increased wear rate regardless of the type of anchorage (cemented or noncemented.[13,14] Polyethylene (PE) wear can easily be detected in polarized light, whereas other wear particles, particularly those from metal alloys, are often missed by histological examination.[15,16] The large numbers of wear particles with a diameter of less than 0.5 μm can only be detected using complex techniques on samples and/or defined areas because of the physical limitations of brightfield and polarized light microscopy.[17–19] Common atom absorption spectrometry methods (AAS, ICP-MS, ICP-OES) used for periprosthetic wear debris analysis demand sample destruction. Thus, a systematic histological assessment of debris accumulation with differentiation between soft and hard tissue is impossible, because bone marrow, soft tissue, and mineralized areas become dissolved and ashed together.[19] Hence, we modified existing preparation procedures and applied a darkfield illumination technique to judge where metal degradation products affect tissue reactions and cause detrimental alterations in periprosthetic bone tissue. Darkfield microscopy is a specialized illumination technique that is characterized by an indirect illumination to increase contrast in specimens that are not imaged well under normal brightfield illumination. Direct light is blocked by an opaque stop in the condenser, whereas light passing through the specimen from oblique angles at all azimuths is diffracted, refracted, and reflected into the objective to form a bright image of the specimen superimposed onto a dark background. The histological allocation of the implant material was verified with proton induced X-ray emission (PIXE) elemental analysis. PIXE was first used in the 1970s for forensic purposes.[20] It has also been used to characterize the implant interface and to demonstrate particulate metals in the periprosthetic environment.[21–23]

MATERIALS AND METHODS

Experimental subjects

Our group of investigators continuously prepares histological sections from joint implants from cadavers for scientific purposes. Five cases without hip replacement revision were selected from this material to investigate the effect of metal degradation products on tissue reactions in the interface regions. Betts et al. suggested that monitoring of debris generation, earlier in the loosening process, may be of great value for studying loosening mechanisms.[24] The prosthesis anchorage was examined using a simple measuring device that measures relative motion greater than 2 μm, under a defined tensile load (100 N), in different directions between implant and bone. Anterior–posterior (AP) X-rays were taken of the implants to evaluate the periprosthetic bone status.

Of the five hip replacements (CrCoMo/PE = chromium cobalt molybdenum/PE), three were cemented (2 × Endo-Modell Mark III, LINK, Hamburg, Germany; 1 × St. Georg Mark II, LINK, Hamburg, Germany) and two noncemented (2 × Spongiosa Metal II, ESKA, Lübeck, Germany). The survival period of the joint replacements varied between 2 and 21 years. All implant-bearers were female (mean age, 75 years). Eight bone biopsies of the iliac crest from eight nonimplant bearers (5 male, 3 female; mean age, 51 years) served as a control group. Hence, the effects of preparation artefacts (band saw blade, microtome knife, etc.) and natural metallic trace elements on darkfield illumination microscopy and microanalysis were taken into account.

Preparation of the histological specimens

All specimens were fixed in buffered formalin (4%). The autopsy and control specimens were prepared and handled as in earlier investigations of femoral components.[25–27] Hence, the proximal femur and the corresponding acetabular region with hip replacements were removed together, keeping the capsule intact. The pelvic tissues were then separated from the femur by a circular incision through the center of the capsule, thus preserving the transition from the capsule to the bone interface.

To investigate the quantity and dissemination of degradation products, sections of tissue, ~4-mm thick, were taken from the lateral, medial, posterior, and anterior regions of the capsule–bone transition area (femur and acetabulum). Cemented PE cups (n = 3) were carefully separated from the bone cement. In addition, four or five horizontal sections and a corresponding number of longitudinal segments were taken from the stem region (Fig. 1). The tissue was processed to ultrathin ground tissue specimens, 15–20-μm thick, using a standard technique as described earlier.[25–27] Glass slides were used instead of plastic, as the optical properties of glass are more suitable for the type of investigation we intended to carry out.

Microscopic darkfield illumination and PIXE microanalysis

The birefringent PE particles in the ground tissue specimens were examined by light-microscopic polarization technique. Nonbirefringent particles, detected under darkfield illumination, were predominantly located in the interface and capsule region and their distribution was

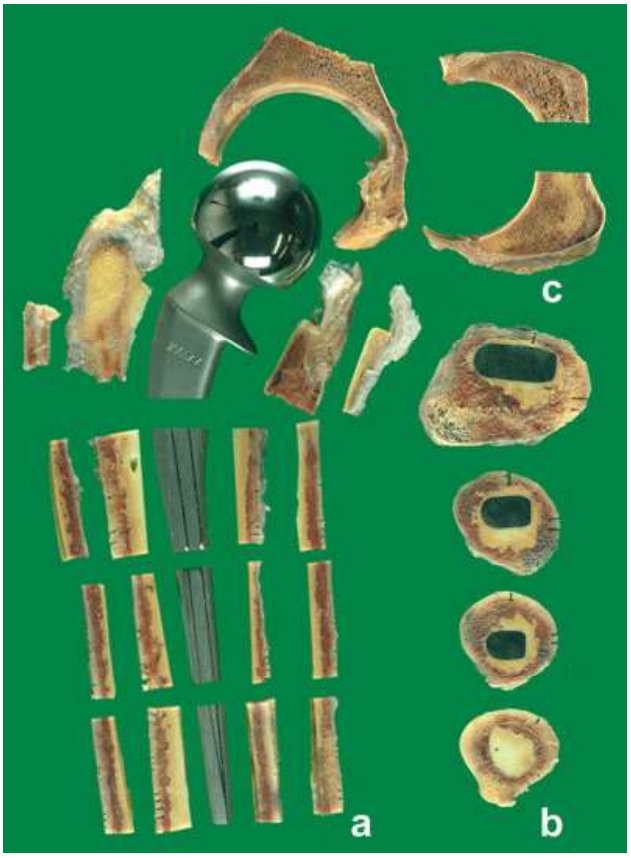

Figure 1. Gross macroscopy: Exemplary preparation of bone tissue in the region of hip replacements, (a) longitudinal segments, (b) horizontal sections, and (c) acetabulum. [Color figure can be viewed in the online issue, which is available at www.interscience.wiley.com.]

recorded. With this type of illumination, very little enlargement is necessary to make wear particles smaller than 0.5 μm visible as luminous points under the microscope (Fig. 2). Sections with high particle density in the medial capsule area/Gruen Zone 7[28] were selected for control identification with elemental analysis [Fig. 3(a)]. High particle density means that a rectangular area of 1.6 mm × 0.8 mm per specimen with a maximum number of visible particles in the soft tissue was chosen [Fig. 3(b,c)]. As the ground tissue specimens were not suitable for the PIXE-technique because of their thickness, new tissue samples had to be taken from the corresponding regions of the remaining material available from the five cases. These were embedded in polymethymethacrylate (PMMA) and then processed to histological undecalcified slices. A 5-μm thick section was stained. A parallel section was re-examined under darkfield and the measurement area marked. This section was then left unstained and fixed with dispersion binder on a slide for microanalysis. The windows of the sample carrier were coated with a 2-μm polycarbonate foil. Measurement of the elemental composition was carried out using PIXE, with a 2-MeV proton microprobe at the Institute for Experimental Physics at the University of Hamburg.[29]

First, the proton beam scanned the chosen rectangular areas of 1.6 mm × 0.8 mm to obtain a general view. Then two detailed readings per area with a field size of 200 μm × 400 μm were analyzed at varying distances to the implant, that is, central and peripheral to the implant [Fig. 3(b,c)]. The probe is sensitive enough to detect extremely small quantities (from 20 ppm), even of lighter elements. The lateral resolution of the PIXE microprobe varies between 1 and 3 μm. The nondestructive analysis of these sections using the PIXE probe enables the direct identification of the metal degradation allocation as seen in the darkfield microscopy.

The specimens from the nonimplant bearer control group were also analyzed with PIXE. The proton beam scanned rectangular areas of 1.6 mm × 0.8 mm to obtain a general view. Then one detailed reading per area with a field size of 200 μm × 400 μm was carried out.

Statistical analysis

A single-sided paired *t*-test was performed to compare the element concentrations central and peripheral to the hip replacement. Values smaller than $p \leq 0.05$ were considered to be significant.

RESULTS

The relative motion measured between implant and bone in the five investigated cases ranged from 3 to 8 μm. Implants within this low range of motion were considered to be firm. The AP X-rays showed neither radiolucent lines nor osteolysis, except one undersized area under the collar of the hip replacement with a 21-year survival. Macroscopic examination of the implants had already shown that, in the three cemented cases, gaps of varying widths (up to 500 μm) were visible between the bone cement and the proximal prosthesis stem. The gaps were mainly located in the medial side and were filled with interface tissue.

The application of brightfield, polarized light, and darkfield microscopy on the control specimens from the nonimplant bearers showed absence of wear products (Fig. 2). Furthermore, microanalysis with PIXE expressed only trace elements and constituents of the bone matrix in these specimens. Detectable elements were calcium (Ca), phosphorus (P), sodium (Na), magnesium (Mg), iron (Fe), zinc (Zn), strontium (Sr), and sulphur (S).

In the implant–bearer group, wear particles were distributed inhomogenously in the tissue. Darkfield microscopy verified by PIXE elemental analysis revealed particle-free areas immediately next to areas with a high particle density (Fig. 3). In darkfield illumination, these areas predominated in the inner medial capsule close to Gruen Zone 7 and

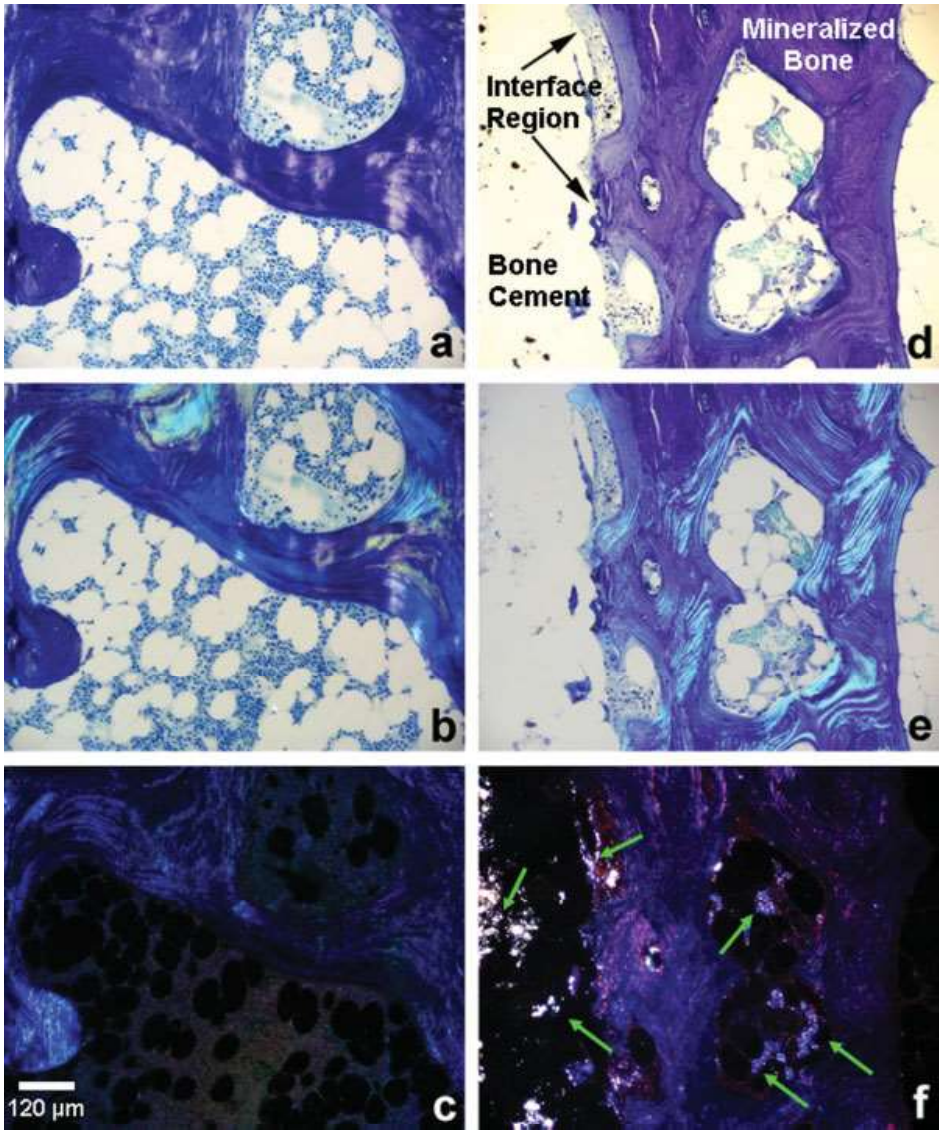

Figure 2. Left column: Control specimen from nonimplant bearer. Under brightfield illumination (a), polarized light (b), and darkfield illumination (c), no metallic particles are visible in the bone tissue. Right column: Specimen from implant-bearer. Small wear particles in periprosthetic bone tissue, which are not visible in brightfield illumination (d) or in partially polarized light (e) are prevalent in darkfield illumination (f) as luminous points in the tissue (arrows), even in low magnification (toluidine blue). [Color figure can be viewed in the online issue, which is available at www.interscience.wiley.com.]

appeared like bright clouds, whereas PE particles do not become visible with this method (Fig. 4).

However, at the interface between cup and bone cement as well as stem and bone cement, some particles were visible in darkfield illumination. These were predominately seen in the connective tissue close to cement mantle defects and within cement fractures extending to the implant surface. PIXE elemental analysis showed that the majority of particles in the capsular tissue of the cemented implants consisted of the radiopaque bone cement constituent zirconia (zirconium dioxide). The synthetic PMMA constituent of the bone cement cannot be measured. The mean size of the eroded zirconium dioxide particles in the capsular tissue was much smaller (0.94 ± 0.61 µm) than the complete zirconia particles in bone cement (13.05 ± 5.25 µm). Large quantities of zirconia were also found within macrophages located at a distance (max. 4 mm) from the capsule and interface [Fig. 5(a–d)]. In contrast, metallic particles were found only in a few macrophages. The measurements yielded the particularly interesting finding that, in the vicinity of implants deposits of cobalt, a heavy metal alloy constituent of the stem/cup component were proven to be deposited in the mineralized bone tissue [Fig. 5(c,e)]. The PIXE spectrum

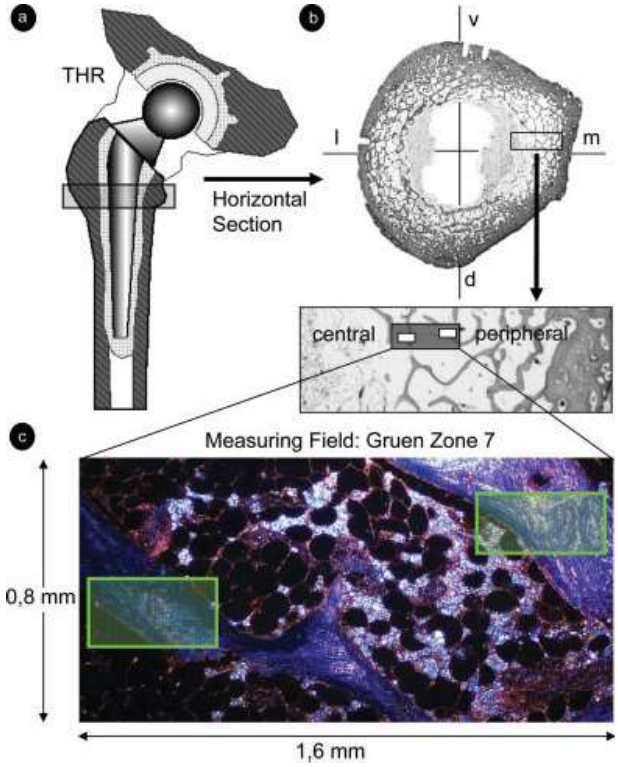

Figure 3. (a) Overview: Removal of the specimen for histological and elemental analysis of the femoral tissue (Gruen Zone 7). (b) Horizontal section (undecalcified, toluidine blue): Medial, a rectangular general view area for element analysis is selected. (c) Two detailed PIXE readings, demonstrating all elements in the measuring field, were quantified centrally and peripherally of the implant (survival: 21 years). [Color figure can be viewed in the online issue, which is available at www.interscience.wiley.com.]

demonstrates all elements in the measuring fields [Fig. 5(f)]. The cobalt concentrations detected in the periprosthetic mineralized bone tissue (Gruen Zone 7) ranged from 38 to 413 ppm [Fig. 6(a,b)]. It was shown that the concentration decreases significantly with increasing distance from the implant [Fig. 6(c)]. However, no cobalt was found in the control group, whereas the highest Co concentrations were detected in the case with an implantation period of over 21 years. We succeeded in analyzing the periarticular bone hard tissue of this case in further detail. Eight additional PIXE analyses proximal and distal of the stem were performed [Fig. 7(a)]. The concentrations of cobalt in the mineralized bone tissue in the proximal region of the stem were significantly higher than in the distal region [Fig. 7(b)]. Other arthroplasty and fixation constituents like chromium, molybdenum, and radiopaque zirconia were not detectable in the mineralized bone tissue.

DISCUSSION

Darkfield microscopy was already used in 1926 to examine spirocheta pallida in cutaneous lesions of secondary syphilis.[30] Willert et al. as well as Raso et al. applied darkfield microscopy for the investigation of silicone deposits in tissues.[31,32] This relatively simple method makes the detection of nonbirefringent particles and conclusions regarding their dissemination feasible, similar to the detection of PE particles under polarized light. In our investigations, darkfield microscopy proved to be an appropriate method for the detection of metallic wear from implants (Fig. 2). It was evident that the quantity of particles present in the tissue was considerably larger than expected, after observation under bright-field illumination with and without polarized light (Fig. 4).

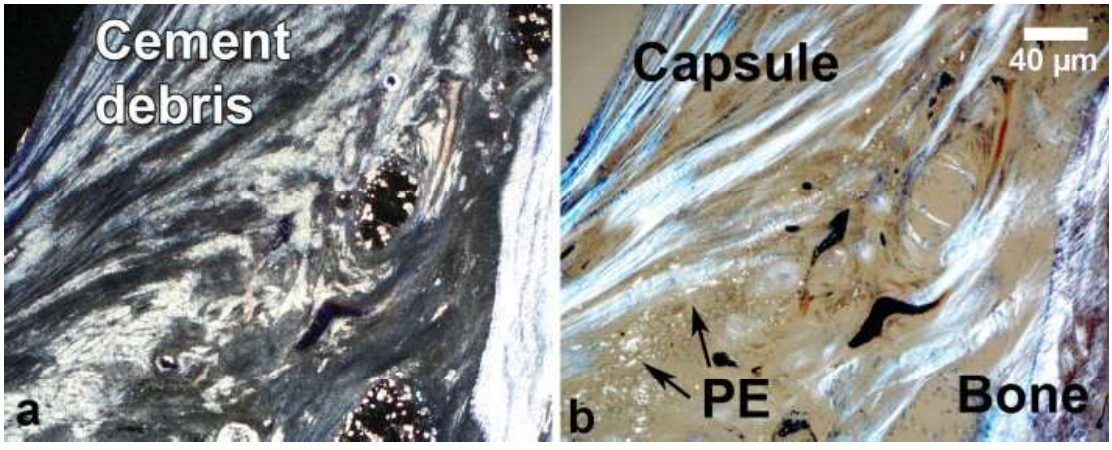

Figure 4. After an implantation period of 6 years, cement particles predominate in the capsular tissue, appearing as bright white clouds, under darkfield illumination (a). The actual extent of particle concentration is not clear in polarized light (b), and only isolated birefringent PE particles (arrow) are visible (toluidine blue). [Color figure can be viewed in the online issue, which is available at www.interscience.wiley.com.]

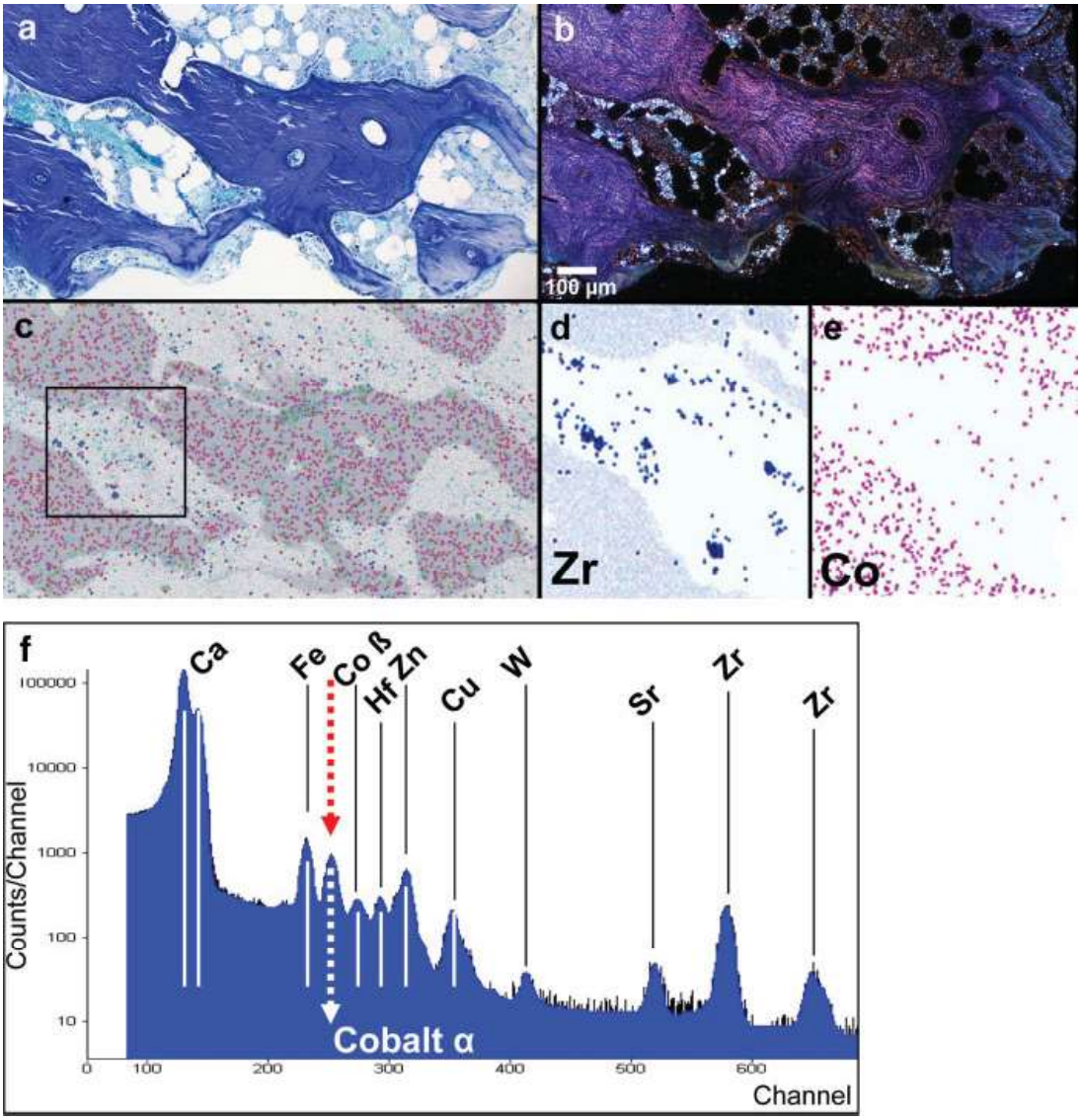

Figure 5. Elemental microanalysis of a histological section (a). Using darkfield microscopy (b), nonbirefringent metal particles within macrophages are visible. PIXE microanalysis shows the elements Ca (grey), Co (purple), Zr (dark blue), Zn (gray), and Fe (light blue) (c). The foreign material in the cells is primarily zirconia (c, d). Higher concentrations of cobalt from the stem/cup component can be detected in the adjacent bone tissue (e), and only very small amounts of chromium are present (toluidine blue). The PIXE spectrum demonstrates all elements in the measuring fields (f). The wolfram peak (W) is an artefact, and it is a component of the microtome knife. Hf (hafnium) is a natural companion of Zr (zirconium). [Color figure can be viewed in the online issue, which is available at www.interscience.wiley.com.]

Using PIXE elemental analysis, we were able to show that the particles found in the tissue around cemented implants originated mostly from constituents of the bone cement. This corresponds to the findings of Bos et al.[33] The size of the eroded zirconia particles in the capsular tissue is substantially lower than in the complete bone cement formation and corresponds approximately to a size relation of 1:14. Zirconia particles can be released by abrasion or break of the synthetic PMMA bone cement component. Since the zirconia particles are obviously smaller in the tissue than in the bone cement, it is likely that the release takes place via a process of wear debris. Furthermore, the gaps between prosthesis stem and cement, observed in the proximal range of the femur, suggest that there is relative motion between the implant components resulting in cement abrasion.

Degradation products of implant materials are known to be detectable in the kidneys, liver, spleen, and lymph nodes,[16,34] or to enter the serum and be finally excreted via the urine.[16,35,36] This is especially true for chromium (Cr) and cobalt (Co). The novel finding of this study was that we obtained unequiv-

a

THR	Original Diagnosis	Fixation	Motion [µm]	Life-time [yrs]	Co [ppm] central	Co [ppm] peripheral
1	coxarthrosis	cementless	firm (5µm)	2	111	87
2	hip fracture	cementless	firm (8µm)	5	60	38
3	coxarthrosis	cemented	firm (3 µm)	6	192	65
4	hip fracture	cemented	firm (5 µm)	7	116	70
5	hip fracture	cemented	firm (7 µm)	21	413	158

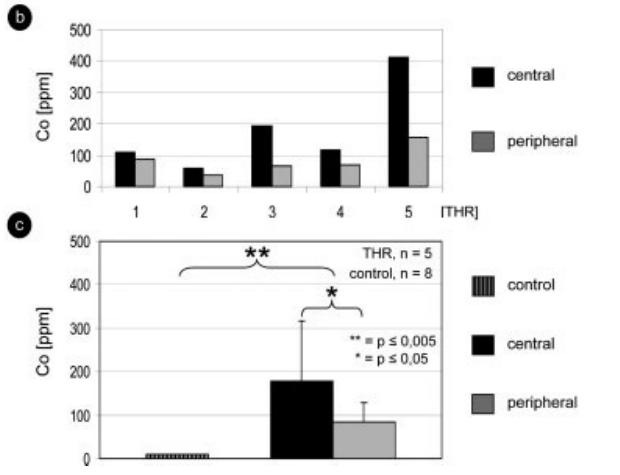

Figure 6. Comparison (a) of the investigated total hip replacements (THR) with original diagnosis, associated motion, service life, fixation type, tribological pairing, and material composition: THR 1-2: ESKA, Spongiosa Metal II; THR 3-4: LINK, Endo-Modell Mark III; THR 5: LINK, St. Georg Mark II. The diagram (b) shows the Co-concentrations in the periprosthetic mineralized bone tissue (Gruen Zone 7) central and peripheral of the implants. In comparison with the control specimen, implant bearers show a significant deposition of cobalt in mineralized bone tissue areas central and peripheral of the implant (c).

ocal evidence that there were larger deposits of cobalt locally in the mineralized bone tissue surrounding joint implants than elsewhere in the skeleton. Other authors performed animal experiments and reported similar findings.[37–39] However, a separate demonstration of the mineralized and nonmineralized bone tissue was not conducted in these studies.

In implant-free bone tissues, as in our control group, cobalt concentrations are below the detection level of the techniques employed in our study. There are indications that the cobalt concentration is related to the distance from the implant. So far, only regions in the immediate vicinity of implants or at a few millimeters distance have been investigated. However, we were able to demonstrate that the implantation of prosthetic material consisting of an ASTM F 75 alloy (~63% Co, 26–30% Cr, 5–7% Mo, ≤1% Ni, ≤1% Mn, ≤0.75% Fe) containing major amounts of cobalt leads to an increase of cobalt concentrations in the periprosthetic mineralized bone tissue. These findings are supported by the descriptions of Dobbs and Minski and Michel et al., who have already reported transportation of cobalt in various body tissues and organs.[40,41]

Darkfield illumination combined with PIXE greatly increases the possibilities for detailed histological assessment of cobalt concentrations. The highest concentrations were detected in the mineralized bone tissue close to the implant (Gruen Zone 7), especially in the case of the implant which survived for over 21 years. The concentration indicates that the deposition of cobalt depends on time and localization. So far, there is no evidence of comparably high concentrations of other alloy constituents in mineralized bone tissue. However, Urban et al. demonstrated

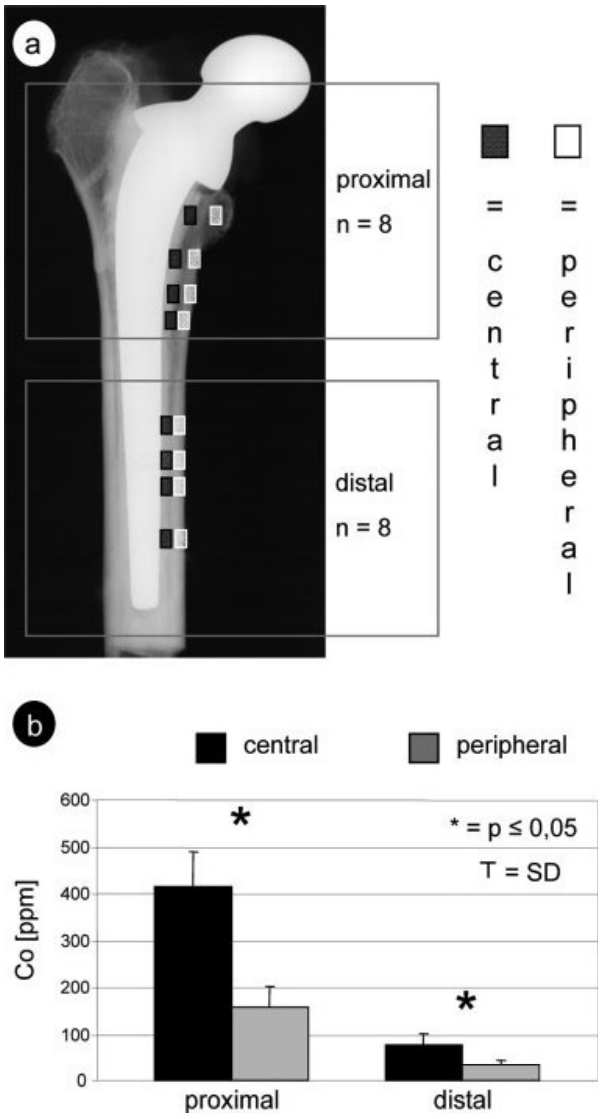

Figure 7. Radiograph (a) of the proximal femur after an implantation period of 21 years (LINK, St. Georg Mark II). The measuring fields in gray and white boxes were evaluated central/peripheral and proximal/distal. The Co-concentrations were significantly higher in the central than in the peripheral region. In the distal periprosthetic regions, the deposition of cobalt is significantly lower (b).

that Cr-orthophosphate was the corrosion product most frequently detected in periprosthetic soft tissue.[42] Furthermore, Willert et al. and Haynes et al. showed in their investigations of CoCr alloys that, during the corrosion process, more cobalt is released than chromium.[43,44] Siddle et al.[45] reported that the Co component in the alloy performs in a similar way to that of the pure metal, which suggests that the cobalt oxidizes independently of the chromium in the alloy. It is therefore conceivable that cobalt is deposited in the bone matrix in a similar way to zinc.[46] However, if the implant particles integrated in the bone matrix are unchanged, it should also be possible to detect the other alloy constituent, chromium. This has succeeded in only a few isolated areas.

It is still unknown if the deposition of cobalt takes place via linked osteocytes or osteoblasts phagocytize particles, which then infiltrate bone tissue during formation of new bone.[47–49] Furthermore, it is still uncertain whether deposition of cobalt in bone tissue is a continuous process, whether it reaches a "saturation point," or whether there is a correlation between the concentration of cobalt and certain lysis zones in the implant bearing.[50] Further investigations will be necessary to determine if a continuous release of alloying components (heavy metals) leads to detrimental alterations and remodeling of mineralized bone tissue. Pathological, for example, tumor-inducing effects on tissue have been discussed by several authors, but causality due to implant degradation has not been proven.[51–55] In this context, Lewold et al. investigated the overall cancer incidence of patients after total knee replacement, but their results do not indicate an increased incidence of cancer following joint replacement.[56] However, prosthesis failure in which the mode of failure leads to metal-on-metal wear or is caused by metal-on-ceramic wear that was not designed to occur can lead to massive tissue metallosis.[57–60] Systemic exposition to cobalt via ingestion, dental treatment, or loose joint replacements can increase susceptibility for local dermatitis due to orthopedic implants or a generalized cobalt-induced dermatitis.[57,61,62] This allergic dermatitis has been discussed by several authors as a consequence of a hapten cross reactivity due to the alloy components cobalt, chromium, and nickel. In the form of haptens they have the potential to generate protein complexes, which can trigger immune reactions. Furthermore, Steens et al. reported chronic cobalt poisoning after hip replacement, which may lead to almost complete loss of sight and hearing.[57]

The potential carcinogenic risk from implants has been evaluated by the International Agency for Research on Cancer. CoCr joint replacements were given a Group 2B classification (possibly carcinogenic in humans).[61,62] Hence, implants with metal-on-metal articulation as well as cobalt-containing prostheses that are anchored without cement should be observed closely. The current analysis leads to the assumption that common implantation techniques lead to the release of cobalt and its incorporation in the surrounding tissue.

Although PIXE elemental analysis is a very sensitive method for nondestructive investigation of histological sections, this highly complex technique is not a routine procedure and therefore cannot be applied to large series.

We thank Mrs. Claudia Kruse and Mrs. Annette Jung for their help with the preparation of the ground tissue specimens.

References

1. Helm CS, Greenwald AS. The rationale and performance of modularity in total hip arthroplasty. Orthopedics 2005;28(9, Suppl):1113–1115.
2. Young AM, Sychterz CJ, Hopper RH Jr, Engh CA. Effect of acetabular modularity on polyethylene wear and osteolysis in total hip arthroplasty. J Bone Joint Surg Am 2002;84:58–63.
3. Hirao M, Sugamoto K, Tamai N, Oka K, Yoshikawa H, Mori Y, Sasaki T. Macro-structural effect of metal surfaces treated using computer-assisted yttrium–aluminum-garnet laser scanning on bone-implant fixation. J Biomed Mater Res A 2005;73:213–222.
4. Krasicka-Cydzik E, Oksiuta Z, Dabrowski JR. Corrosion testing of sintered samples made of the Co—Cr—Mo alloy for surgical applications. J Mater Sci Mater Med 2005;16:197–202.
5. Placko HE, Brown SA, Payer JH, Effects of microstructure on the corrosion behavior of CoCr porous coatings on orthopedic implants. J Biomed Mater Res 1998;39:292–299.
6. Berry DJ, Harmsen WS, Cabanela ME, Morrey BF. Twenty-five-year survivorship of two thousand consecutive primary Charnley total hip replacements: Factors affecting survivorship of acetabular and femoral components. J Bone Joint Surg Am 2002;84:171–177.
7. Heisel C, Silva M, Schmalzried TP. Bearing surface options for total hip replacement in young patients. Instr Course Lect 2004;53:49–65.
8. Katzer A, Hockertz S, Buchhorn GH, Loehr JF. In vitro toxicity and mutagenicity of CoCrMo and Ti6Al wear particles. Toxicology 2003;190:145–154.
9. Older J. Charnley low-friction arthroplasty: A worldwide retrospective review at 15 to 20 years. J Arthroplasty 2002;17: 675–680.
10. Engelbrecht E, Hahn M. Socket wear in the St. Georg hip prosthesis after long-term service. In: Willert HG, Buchhorn GH, Eyerer P, editors. Ultra-High Molecular Weight Polyethylene as Biomaterial in Orthopedic Surgery. Toronto: Hogrefe & Huber; 1991. p 143–147.
11. Sundfeldt M, Carlsson LV, Johansson CB, Thomsen P, Gretzer C. Aseptic loosening, not only a question of wear: A review of different theories. Acta Orthop 2006;77:177–197.
12. Willert H-G. Differences and similarities of osteolyses from particulate polyethylene and PMMA-bone cement. In: Willert HG, Buchhorn GH, Eyerer P, editors. Ultra-High Molecular Weight Polyethylene as Biomaterial in Orthopedic Surgery. Toronto: Hogrefe & Huber; 1991. p 89–103.
13. Dunstan E, Sanghrajka AP, Tilley S, Unwin P, Blunn G, Cannon SR, Briggs TW. Metal ion levels after metal-on-metal

proximal femoral replacements: A 30-year follow-up. J Bone Joint Surg Br 2005;87:628–631.
14. Massin P, Chappard D, Flautre B, Hardouin P. Migration of polyethylene particles around nonloosened cemented femoral components from a total hip arthroplasty—An autopsy study. J Biomed Mater Res B Appl Biomater 2004;69:205–215.
15. Bos I, Lindner B, Seydel U, Johannisson R. Identification of wear particles of joint prostheses in tissues using laser microprobe mass analysis (LAMMA). Biomed Tech (Berl) 2001; 46:253–258.
16. Urban RM, Jacobs JJ, Tomlinson MJ, Gavrilovic J, Black J, Peoc'h M. Dissemination of wear particles to the liver, spleen, and abdominal lymph nodes of patients with hip or knee replacement. J Bone Joint Surg Am 2000;82:455–456.
17. Bos I. Tissue reactions around loosened hip joint endoprostheses. A histological study of secondary capsules and interface membranes. Orthopade 2001;30:881–889.
18. Maloney WJ, Smith RL, Schmalzried TP, Chiba J, Huene D, Rubash H. Isolation and characterization of wear particles generated in patients who have had failure of a hip arthroplasty without cement. J Bone Joint Surg Am 1995;77:1301–1310.
19. Salvati EA, Betts F, Doty SB. Particulate metallic debris in cemented total hip arthroplasty. Clin Orthop Relat Res 1993; Aug (293):160–173.
20. Lindh U, Brune D, Nordberg G. Microprobe analysis of lead in human femur by proton induced X-ray emission (PIXE). Sci Total Environ 1978;10:31–37.
21. Frayssinet P, Braye F, Weber G. Analysis of sections of implanted macroporous calcium phosphate bone substitutes by proton-induced X-emission method and energy-dispersive spectrometry. Scanning 1997;19:253–257.
22. Jallot E. Correlation between hydroxyapatite osseointegration and Young's Modulus. Med Eng Phys 1998;20:697–701.
23. Passi P, Zadro A, Galassini S, Rossi P, Moschini G. PIXE micro-beam mapping of metals in human peri-implant tissues. J Mater Sci Mater Med 2002;13:1083–1089.
24. Betts F, Wright T, Salvati EA, Boskey A, Bansal M. Cobalt-alloy metal debris in periarticular tissues from total hip revision arthroplasties. Metal contents and associated histologic findings. Clin Orthop Relat Res 1992;Mar (276):75–82.
25. Hahn M, Vogel M, Schulz C, Niecke M, Delling G. Histologic reactions of the bone-implant zone and cortical bone area after long-term hip replacement. Chirurg 1992;63:958–963.
26. Hahn M. Quantitative analysis of the histological reactions at the interface and the surrounding bone tissue following the implantation of hip endoprostheses. In: Barbosa MA, Campilho A, editors. Imaging Techniques in Biomaterials. North-Holland: Elsevier; 1994. p 325–340.
27. Hahn M, Vogel M, Delling G. Undecalcified preparation of bone tissue: Report of technical experience and development of new methods. Virchows Arch A Pathol Anat Histopathol 1991;418:1–7.
28. Gruen TA, McNeice GM, Amstutz HC. Modes of failure of cemented stem-type femoral components: A radiographic analysis of loosening. Clin Orthop Relat Res 1979;Jun (141): 17–27.
29. Niecke M. PIXE-Pikogramm-Protonenmikrosonde. Spurenelementanalytik durch Protonen-induzierte Emission von Röntgenstrahlung. Labor 1991;2000:94–102.
30. Templeton HJ. The value of darkfield microscopy in the differential diagnosis of secondary syphilis. Calif West Med 1926;25:623.
31. Willert HG, Buchhorn G, Semlitsch M. Tissue reaction to abrasion of upper extremity joint endoprostheses. Orthopade 1980; 9:94–107.
32. Raso DS, Green WB, Vesely JJ, Willingham MC. Light microscopy techniques for the demonstration of silicone gel. Arch Pathol Lab Med Ost 1994;118:984–987.
33. Bos I, Friedebold D, Diebold J, Löhrs U. Tissue reaction to cemented hip sockets. Histologic and morphometric autopsy study of 25 acetabula. Acta Orthop Scand 1995;66:1–8.
34. Urban RM, Tomlinson MJ, Hall DJ, Jacobs JJ. Accumulation in liver and spleen of metal particles generated at nonbearing surfaces in hip arthroplasty. J Arthroplasty 2004;19(8, Suppl 3): 94–101.
35. Bartolozzi A, Black J. Chromium concentration in serum, blood clot and urine from patients following total hip arthroplasty. Biomaterials 1985;6:2–8.
36. Jacobs JJ, Skipor AK, Patterson LM, Hallab NJ, Paprosky WG, Black J, Galante JO. Metal release in patients who have had a primary total hip arthroplasty. A prospective, controlled, longitudinal study. J Bone Joint Surg Am 1998;80:1447–1458.
37. Flodh H. Autoradiographic studies on distribution of radiocobalt chloride in pregnant mice. Acta Radiol Ther Phys Biol 1968;7:121–128.
38. Soremark R, Diab M, Arvidson K. Autoradiographic study of distribution patterns of metals which occur as corrosion products from dental restorations. Scand J Dent Res 1979;87: 450–458.
39. Okazaki Y, Gotoh E, Manabe T, Kobayashi K. Comparison of metal concentrations in rat tibia tissues with various metallic implants. Biomaterials 2004;25:5913–5920.
40. Dobbs HS, Minski MJ. Metal ion release after total hip replacement. Biomaterials 1980;1:193–198.
41. Michel R, Nolte M, Reich M, Loer F. Systemic effects of implanted prostheses made of cobalt–chromium alloys. Arch Orthop Trauma Surg 1991;110:61–74.
42. Urban RM, Jacobs JJ, Gilbert JL, Galante JO. Migration of corrosion products from modular hip prostheses. Particle microanalysis and histopathological findings. J Bone Joint Surg Am 1994;76:1345–1359.
43. Willert HG, Buchhorn GH, Gobel D, Koster G, Schaffner S, Schenk R, Semlitsch M. Wear behavior and histopathology of classic cemented metal on metal hip endoprostheses. Clin Orthop Relat Res 1996;Aug (329):S160–S186.
44. Haynes DR, Crotti TN, Haywood MR. Corrosion of and changes in biological effects of cobalt chrome alloy and 316-L stainless steel prosthetic particles with age. J Biomed Mater Res 2000;49:167–175.
45. Siddle A, Castle JE, Hultquist G, Tan KL. Investigation of the initial reaction of the alloy Co86Cr14 and its constituent metals with oxygen using secondary ion mass spectrometry. Surf Interface Anal 2002;33:807–814.
46. Samachson J, Dennis J, Fowler R, Schmitz A. The Reaction of. ^{65}Zn with the surfaces of bone and bone mineral. Biochim Biophys Acta 1967;148:767–773.
47. Lohmann CH, Schwartz Z, Koster G, Jahn U, Buchhorn GH, MacDougall MJ, Casasola D, Liu Y, Sylvia VL, Dean DD, Boyan BD. Phagocytosis of wear debris by osteoblasts affects differentiation and local factor production in a manner dependent on particle composition. Biomaterials 2000;21:551–561.
48. Lohmann CH, Dean DD, Koster G, Casasola D, Buchhorn GH, Fink U, Schwartz Z, Boyan BD. Ceramic and PMMA particles differentially affect osteoblast phenotype. Biomaterials 2002;23:1855–1863.
49. Rahbek O, Kold S, Bendix K, Overgaard S, Soballe K. No effect of hydroxyapatite particles in phagocytosable sizes on implant fixation: An experimental study in dogs. J Biomed Mater Res A 2005;73:150–157.
50. Cobb AG, Schmalzreid TP. The clinical significance of metal ion release from cobalt–chromium metal-on-metal hip joint arthroplasty. Proc Inst Mech Eng [H] 2006;220:385–398.